Lithium–Sulfur Batteries

Deutsche Ausgabe: DOI: 10.1002/ange.201609147
Internationale Ausgabe: DOI: 10.1002/anie.201609147

Ferrocene-Promoted Long-Cycle Lithium–Sulfur Batteries

Yingying Mi[+], Wen Liu[+], Ke R. Yang[+], Jianbing Jiang, Qi Fan, Zhe Weng, Yiren Zhong, Zishan Wu, Gary W. Brudvig, Victor S. Batista, Henghui Zhou,* and Hailiang Wang**

Abstract: *Confining lithium polysulfide intermediates is one of the most effective ways to alleviate the capacity fade of sulfur-cathode materials in lithium–sulfur (Li–S) batteries. To develop long-cycle Li–S batteries, there is an urgent need for material structures with effective polysulfide binding capability and well-defined surface sites; thereby improving cycling stability and allowing study of molecular-level interactions. This challenge was addressed by introducing an organometallic molecular compound, ferrocene, as a new polysulfide-confining agent. With ferrocene molecules covalently anchored on graphene oxide, sulfur electrode materials with capacity decay as low as 0.014 % per cycle were realized, among the best of cycling stabilities reported to date. With combined spectroscopic studies and theoretical calculations, it was determined that effective polysulfide binding originates from favorable cation–π interactions between Li^+ of lithium polysulfides and the negatively charged cyclopentadienyl ligands of ferrocene.*

Lithium-based rechargeable battery systems are important power sources and energy-storage devices. Given that the low capacity of the traditional cathode materials (ca. 170 mAh g^{-1} for $LiFePO_4$ and ca. 150 mAh g^{-1} for layered metal oxides) limits battery performance,[1] researchers are motivated to locate new cathode materials with higher capacity. Sulfur is a promising candidate owing to its high theoretical specific capacity (1675 mAh g^{-1}), high abundance, and non-toxicity.[2] Lithium–sulfur (Li–S) batteries have thus become a research hotspot in the past decade. Nonetheless, short-cycle life continues to impede the existing Li–S batteries. One pivotal cause of this phenomenon is the well-known shuttle effect of the soluble lithium polysulfide intermediates (Li_2S_x, $4 \leq x \leq 8$).[3]

Many materials to date, including heteroatom-doped carbons,[4] polymer-based materials,[5] metal oxides,[6] and metal chalcogenides,[7] have been demonstrated to be effective for confining lithium polysulfides. For example, the groups of Nazar and Cui have utilized titanium oxides to immobilize polysulfides and achieved sulfur electrodes with capacity decay as low as 0.033 % per cycle;[6c,8] Zhang's group resorted to CoS_2 for binding polysulfides, and a slow capacity fading rate of 0.034 % per cycle was realized.[7b] Nevertheless, the majority of these host materials are inorganic solids, of which only the surface atoms can possibly be used as active sites for polysulfide trapping. Additionally, inorganic solid materials often have many types of surface sites, making it difficult to discern the interaction mechanisms. With these concerns in mind, we consider metal–organic complexes as more efficient polysulfide-confining materials because they can be dispersed as individual molecules on a surface. They are also a more suitable model system to elucidate the underlying surface-binding mechanism because of their well-defined molecular structures.

Reported for the first time, herein we describe use of ferrocene (Fc; a commonly used organometallic compound consisting of two cyclopentadienyl (Cp) rings bound to an iron atom)[9] as a polysulfide-confining agent to promote long-cycle Li–S batteries. Fc and many of its derivatives are commercially available and can be linked with relative ease to carbon materials (such as graphene) using known chemistry.[10] We find that Fc non-covalently attached to graphene oxide (GO) is effective for suppressing lithium polysulfide shuttling and consequently capacity fading. Covalently linking Fc molecules to GO can further optimize electrochemical performance. With a sulfur content of 73 wt %, the material exhibits exceptional cycling stability with 0.014 % capacity decay per cycle over 550 cycles. Density functional theory (DFT) calculations suggest that the anchored Fc groups bind lithium polysulfides as a consequence of interactions between the Cp rings and the lithium ions, which is confirmed by X-ray photoelectron spectroscopy (XPS) studies.

Fc was firstly attached to GO non-covalently (GO-nc-Fc), by π–π stacking, based on a previously reported method.[11] Scanning electron microscopy (SEM; Supporting Information, Figure S1d), transmission electron microscopy (TEM) imaging (Figure 1a; Supporting Information, Figure S1e), and energy-dispersive X-ray spectroscopy (EDX) elemental mapping (Supporting Information, Figure S1g,h,i) reveal that Fc clusters with a size of about 3 nm are uniformly distributed on GO layers (Supporting Information, Figure S1a,b), consistent with the previous results.[11] Strong iron peaks were recorded in the EDX spectrum (Figure 1b), suggesting that Fc is anchored on GO. The iron content in the material is calculated to be approximately 17 wt %. Fc attachment is further confirmed by CV characterization, where a pair of redox peaks characteristic of Fc are identified in the potential

[*] Y. Mi,[+] Dr. W. Liu,[+] Dr. K. R. Yang,[+] Dr. J. Jiang, Dr. Z. Weng, Y. Zhong, Z. Wu, Prof. G. W. Brudvig, Prof. V. S. Batista, Prof. H. Wang
Department of Chemistry and Energy Sciences Institute
Yale University
810 West Campus Drive, West Haven, CT 06516 (USA)
E-mail: victor.batista@yale.edu
hailiang.wang@yale.edu

Y. Mi,[+] Prof. H. Zhou
College of Chemistry and Molecular Engineering, Peking University
Beijing 100871 (China)
E-mail: hhzhou@pku.edu.cn

Dr. Q. Fan
School of Chemistry and Chemical Engineering, Southeast University
Nanjing, Jiangsu 211189 (China)

[+] These authors contributed equally to this work.

Supporting information for this article can be found under: http://dx.doi.org/10.1002/anie.201609147.

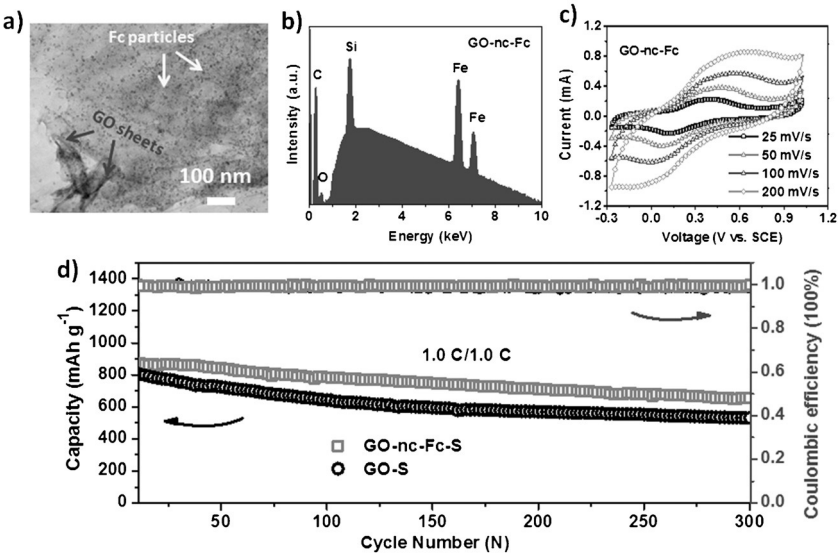

Figure 1. Characterization of Fc functionalized GO assembled with non-covalent bonding (GO-nc-Fc). a) TEM image of GO-nc-Fc. b) EDX spectrum of GO-nc-Fc. c) CV curves of GO-nc-Fc in 0.1 mol L^{-1} PBS at pH 7.4. d) Long-term cycling performance of GO-nc-Fc-S compared with GO-S. Sulfur content is about 62 wt% in the electrode materials.

range (Figure 1c; Supporting Information, Figure S2). No obvious diffraction peaks appear in the XRD pattern of the material (Supporting Information, Figure S3a), excluding formation of iron oxide crystallites. The Raman spectrum of GO-nc-Fc features a D band (1350 cm^{-1}) and a G band (1580 cm^{-1}) with smaller peak widths and a higher I_D/I_G ratio compared to GO itself (Supporting Information, Figure S3b), indicating that the GO is partially reduced during the Fc functionalization process. The reduction is probably caused by DMF, which is known to reduce GO under similar conditions.[12]

Sulfur was then uniformly deposited on GO-nc-Fc by the Na_2S_x decomposition method[13] (GO-nc-Fc-S; Supporting Information, Figure S1f). With a sulfur content of about 62 wt%, the GO-nc-Fc-S material exhibits good specific capacity and rate capability, together with characteristic discharging–charging voltage profiles (Supporting Information, Figure S4a,c), comparable to sulfur directly deposited on GO (GO-S; Supporting Information, Figure S1c and Figure S4b,c). Specific capacities of 1205 and 902 mAh g^{-1} were obtained at 0.2 and 1.0 C for GO-nc-Fc-S. Incorporation of Fc in the material structure considerably increased cycling stability. The average capacity fading for the GO-nc-Fc-S electrode

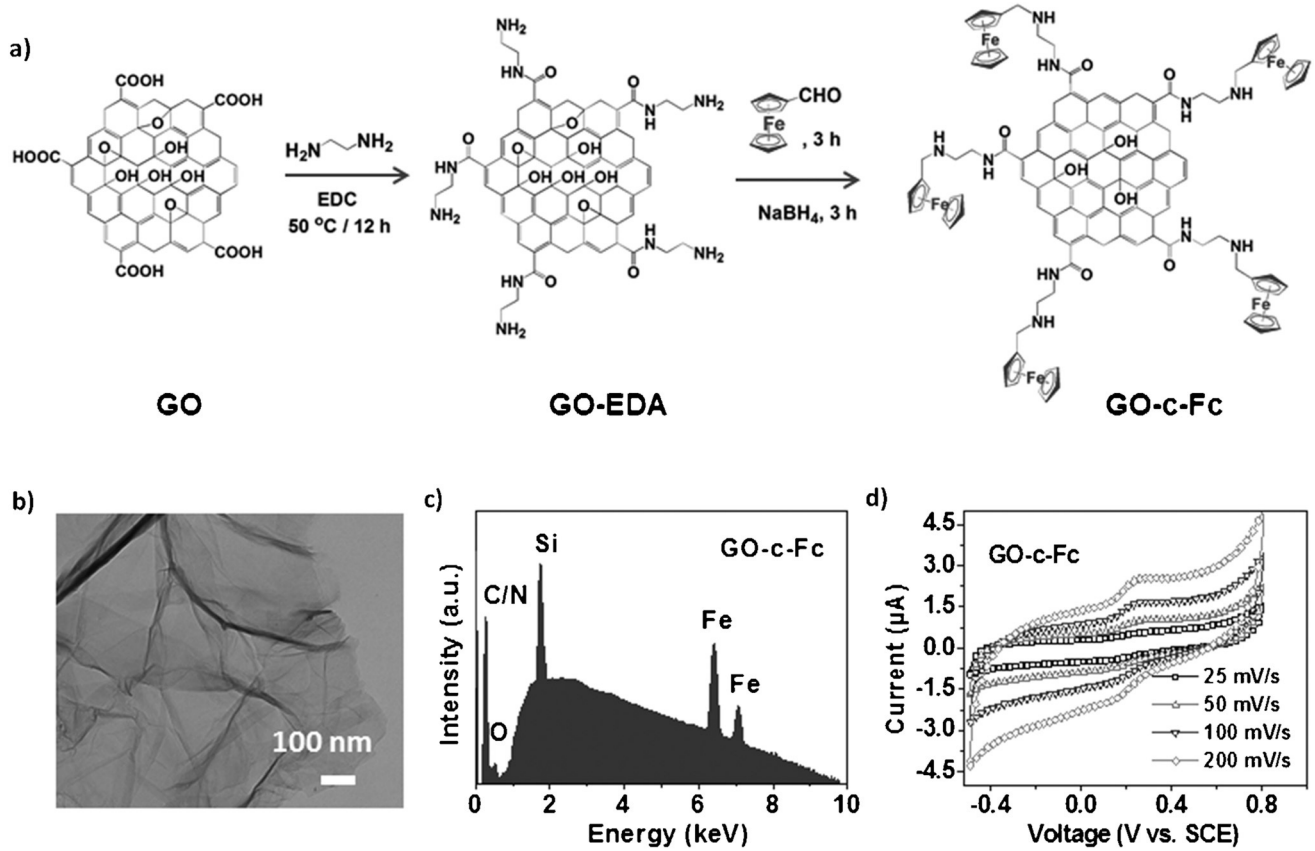

Figure 2. Synthesis and characterization of Fc functionalized GO assembled with covalent bonding (GO-c-Fc). a) Synthesis of GO-c-Fc. b) TEM image of GO-c-Fc. c) EDX spectrum of GO-c-Fc. d) CV curves of GO-c-Fc in 0.1 mol L^{-1} PBS at pH 7.4.

was 0.07% per cycle over the first 300 recharging cycles, as compared to 0.12% capacity decay per cycle for the GO-S material (Figure 1d).

With the aim to fully realize the potential of Fc for polysulfide confinement, we considered an alternative approach to functionalization of GO with Fc: forming covalent chemical bonds. Covalent linkers are stronger than non-covalent interactions and are thus more resistant against Fc detaching from GO under battery operation conditions. Furthermore, covalent functionalization can provide a molecular-level distribution of Fc on GO, which improves the utilization of the Fc molecules. Our synthetic route to covalently anchored Fc on GO (GO-c-Fc) is shown in Figure 2a. Ethylenediamine (EDA) was first linked to GO by reacting the amino groups of EDA with the carboxylic groups of GO. Subsequently, GO-EDA was further decorated with Fc groups using the reaction between the amino groups of GO-EDA and the aldehyde groups of ferrocenecarboxaldehyde to afford the final material, GO-c-Fc. GO-c-Fc was characterized by a series of techniques and the results are shown in Figure 2. No discernable particles were observed on GO by SEM (Supporting Information, Figure S5a) and TEM (Figure 2b; Supporting Information, Figure S5b), suggesting that the Fc molecules are linked to GO without forming aggregates, as opposed to the non-covalent assembly described above. EDX elemental mapping confirms the uniform distribution of Fc on GO (Supporting Information, Figure S5d,e,f). The existence of Fc on the GO surface is clearly verified by the iron peaks in the EDX spectrum (Figure 2c) and is further supported by the CV curves where the characteristic Fc Faradaic redox peaks are clearly superimposed on the capacitive responses from GO (Figure 2d). Notably,
GO-c-Fc contains less Fc than GO-nc-Fc, as indicated by a lower Fe/C intensity ratio in the EDX spectrum (Figure 2c) and weaker Fc redox peaks in the CV curves (Figure 2d). The iron content in the material is approximately 10 wt%, based on the EDX analysis. The GO in the GO-c-Fc was also partially reduced (Supporting Information, Figure S6b), likely as a result of the excess $NaBH_4$ used in the synthesis.[14]

After sulfur deposition, the GO-c-Fc-S material (Supporting Information, Figure S5c) with a sulfur content of approximately 62 wt% manifests remarkable electrochemical performance as a cathode material in a Li–S battery. The specific capacities at various rates, and the corresponding discharging–charging voltage profiles are shown in Figure 3a,b. Specific capacities of 1179, 1006, 903, and 724 mAh g^{-1} were obtained at 0.2, 0.5, 1.0, and 2.0C, respectively, demonstrating good rate capability that is comparable to other reported high-performance sulfur-cathode materials.[4d,6c,15] Notably, GO-c-Fc-S shows superior cycling stability, with 0.03% capacity decay per cycle over 500 cycles (Figure 3c). The Coulombic efficiency stays above 98.8% during cycling, which outperforms GO-nc-Fc-S with a capacity decrease of 0.06% per cycle over 500 cycles. Electrochemical impedance spectroscopy (EIS) measurements were performed for the GO-c-Fc-S, GO-nc-Fc-S, and GO-S materials in their corresponding Li–S cells, before and after cycling. It is evident that Fc is highly effective in

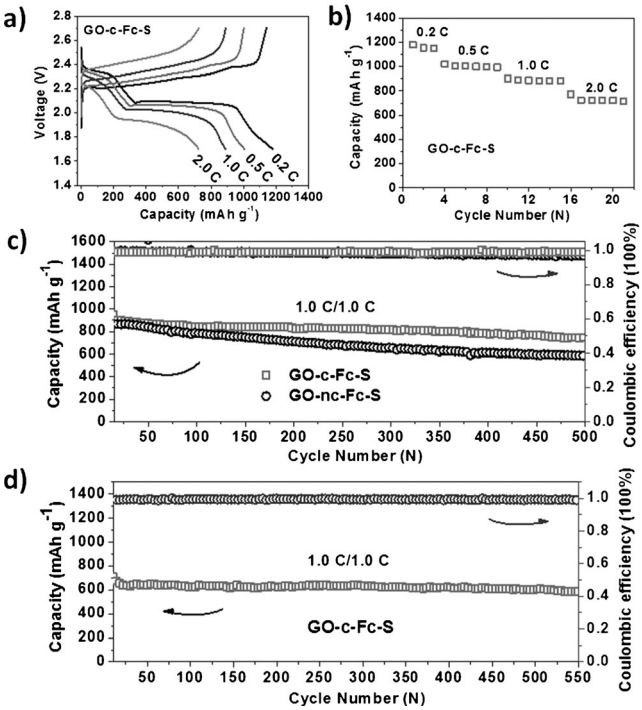

Figure 3. Electrochemical performance of GO-c-Fc-S as the cathode for Li–S batteries. a) Representative discharging–charging voltage profiles of GO-c-Fc-S at 0.2, 0.5, 1.0, and 2.0C. b) Rate capability of GO-c-Fc-S. c) Long-cycle performance of GO-c-Fc-S at 1.0C compared with GO-nc-Fc-S. The sulfur content of the electrode materials in (a–c) is about 62 wt%. d) Long-cycle performance of GO-c-Fc-S at 1.0C, with a sulfur content of about 73 wt% in the electrode material.

suppressing the increase of charge transfer resistance over cycling (Supporting Information, Figure S7), likely because of the polysulfide-confining capability of Fc. The results agree very well with the observed cycling stability of the three materials.

As the sulfur content increases to 73 wt%, GO-c-Fc-S shows even better cycling stability despite a compromised rate capability (Supporting Information, Figure S8a,b). Capacity fading is as slow as 0.014% per cycle over 550 cycles (Figure 3d; from 638 mAh g^{-1} at the 10th cycle, to 588 mAh g^{-1} at the 550th cycle) with a Coulombic efficiency over 98.2%, representing one of the most stable sulfur-cathode materials reported to date.[6c,16] Even at a high sulfur mass loading of 4 mg cm^{-2} on the electrode, GO-c-Fc-S still works well with a specific capacity as high as 740 mAh g^{-1} (corresponding to an areal capacity of 3 mAh cm^{-2}), which is retained after 100 cycles at 0.2C (Supporting Information, Figure S9). Coulombic efficiency is higher than 98% throughout cycling. The results clearly demonstrate the effectiveness of the covalently anchored Fc molecules for confining polysulfides and improving battery cycle life. As a control, the GO-EDA-S material without Fc exhibits significantly inferior cycling stability (0.08% capacity decay per cycle; Supporting Information, Figure S8) compared with that of GO-c-Fc-S.

XPS studies were performed to probe the chemical interactions between Fc and lithium polysulfides. Li_2S_4 was

employed as a representative polysulfide species. The S 2p core level spectrum of free Li_2S_4 exhibits terminal (S_T^{-1} at 161.4 and 162.6 eV) and bridging (S_B^0 at 163.0 and 164.2 eV) sulfur components in a ratio of about 1:1 (Figure 4a), which agrees well with previous reports.[17] In comparison, the S 2p components shift to higher binding energies for Li_2S_4 adsorbed on GO-c-Fc (Figure 4a). Concomitantly, the Fe 2p components shift to higher binding energies upon Li_2S_4 adsorption (Figure 4b). The shifts are attributed to the interaction between Fc and Li_2S_4. Similar changes in S 2p and Fe 2p core level spectra were also observed for Li_2S_4 adsorbed on GO-nc-Fc (Supporting Information, Figure S10a,b). For both GO-c-Fc and GO-nc-Fc, the binding energy of O 1s core level electrons does not shift upon Li_2S_4 adsorption (Figure 4c; Supporting Information, Figure S10c), indicating no strong interaction between Li_2S_4 and GO.[17] The results thus confirm that lithium polysulfides preferentially bind to Fc in our materials.

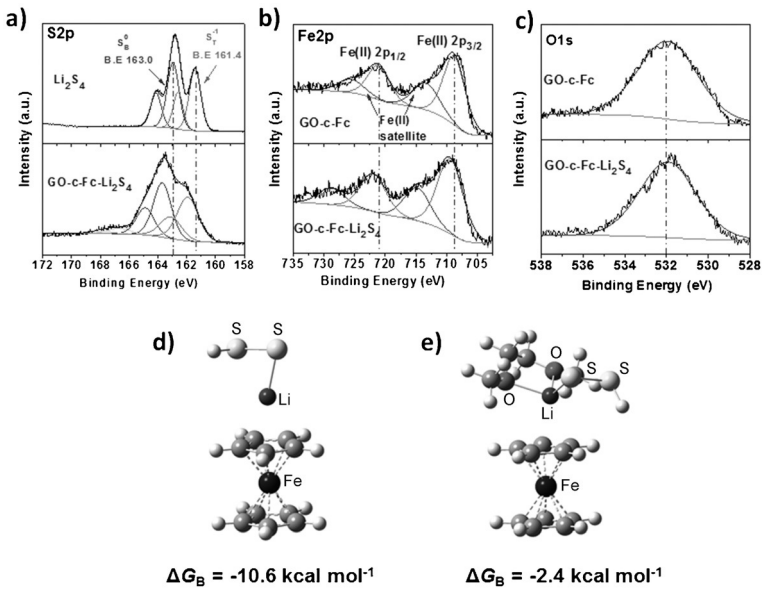

Figure 4. XPS and DFT study of the interactions between Li_2S_4 and GO-c-Fc. a) S 2p core level spectra of free Li_2S_4 and Li_2S_4 adsorbed on GO-c-Fc. b) Fe 2p and c) O 1s core level spectra of GO-c-Fc and GO-c-Fc with adsorbed Li_2S_4. Optimized structures and binding free energy changes (ΔG_B) of d) free LiSSH and e) DME solvated LiSSH interacting with Fc.

DFT calculations provide insights on fundamental interactions between lithium polysulfides and Fc. LiSSH was chosen as a model of lithium polysulfide compounds in our simulations. We find that direct Fe-S interactions (Supporting Information, Scheme S1) are disfavored since they require displacement of a Cp ring from Fc. However, cation–π interactions[18] between the Li^+ of LiSSH and the Cp ring of Fc are very favorable, as revealed by DFT free energy calculations of the binding strength (ΔG_B) between LiSSH and Fc:

$$\Delta G_B = G(\mathrm{HSSLiSol_m FeCp_2}) - G(\mathrm{HSSLiSol_m}) - G(\mathrm{FeCp_2})$$

where $HSSLiSol_m$ represents solvated LiSSH (with m solvent molecules), $FeCp_2$ is Fc, and $HSSLiSol_mFeCp_2$ is the complex of the two. Neglecting the effect of solvation, we find that LiSSH binds to Fc quite strongly with $\Delta G_B = -10.6$ kcal mol^{-1} (Figure 4d), and in dimethoxyethane (DME) the binding is still quite significant ($\Delta G_B = -2.4$ kcal mol^{-1}; Figure 4e). The analysis of optimized geometries shows that lithium polysulfides can be confined by Fc by direct interactions between the negatively charged Cp ring and Li^+. These results are consistent with previous studies showing that Fc interacts strongly with Li^+ through cation–π interactions.[18,19] In fact, several Li–Fc complexes have been experimentally isolated,[19a–c] and our calculated structure (Figure 4e) resembles the crystal structure of a DME solvated Li–Fc complex.[19b]

In summary, we have investigated Fc as a lithium polysulfide-confining agent for Li–S batteries with remarkable performance. We find that Fc molecules covalently linked to GO nanosheets yield sulfur-cathode materials with outstanding cycling stability. The well-defined molecular structure of Fc also facilitates mechanistic studies. The DFT computational analysis, in combination with XPS characterization, reveals that lithium polysulfides bind to Fc through cation–π interactions between Li^+ and the Cp ring, enabling a long-cycle life when implemented in Li–S batteries.

Acknowledgements

This work is partially supported by Yale University. Y.M. is thankful for support from China Scholarship Council (CSC). Computational and synthetic work was supported by the U.S. Department of Energy Office of Science, Office of Basic Energy Sciences, under award no. DE-FG02-07ER15909, and by a generous donation from the TomKat Charitable Trust. We appreciate the assistance of Min Li (Materials Characterization Core, Yale University) with materials characterization. V.S.B. acknowledges funding from the Argonne-Northwestern Solar Energy Research (ANSER) Center, an Energy Frontier Research Center funded by the U.S. Department of Energy, Office of Science, Office of Basic Energy Sciences, under award no. DE-PS02-08ER15944, and computer time from National Energy Research Scientific Computing Center (NERSC) and Yale High Performance Computation Center.

Keywords: ferrocene · graphene oxide · lithium polysulfides · lithium–sulfur batteries · long-cycle batteries

How to cite: *Angew. Chem. Int. Ed.* **2016**, *55*, 14818–14822
Angew. Chem. **2016**, *128*, 15038–15042

[1] a) N. S. Choi, Z. H. Chen, S. A. Freunberger, X. L. Ji, Y. K. Sun et al., *Angew. Chem. Int. Ed.* **2012**, *51*, 9994–10024; *Angew. Chem.* **2012**, *124*, 10134–10166; b) J. M. Tarascon, M. Armand, *Nature* **2001**, *414*, 359–367.

[2] a) Y. X. Yin, S. Xin, Y. G. Guo, L. J. Wan, *Angew. Chem. Int. Ed.* **2013**, *52*, 13186–13200; *Angew. Chem.* **2013**, *125*, 13426–13441;

b) X. Ji, L. F. Nazar, *J. Mater. Chem.* **2010**, *20*, 9821 – 9826; c) D. Lv, J. Zheng, Q. Li, X. Xie, S. Ferrara et al., *Adv. Energy Mater.* **2015**, *5*, 1402290.

[3] a) Y. V. Mikhaylik, J. R. Akridge, *J. Electrochem. Soc.* **2004**, *151*, A1969 – A1976; b) M. U. M. Patel, R. Demir Cakan, M. Morcrette, J. M. Tarascon, M. Gaberscek et al., *ChemSusChem* **2013**, *6*, 1177 – 1181; c) X. Yu, H. Pan, Y. Zhou, P. Northrup, J. Xiao et al., *Adv. Energy Mater.* **2015**, *5*, 1500072.

[4] a) G. Zhou, Y. Zhao, A. Manthiram, *Adv. Energy Mater.* **2015**, *5*, 1402263; b) Z. Wang, Y. Dong, H. Li, Z. Zhao, H. Bin Wu et al., *Nat. Commun.* **2014**, *5*, 5002; c) J. Song, M. L. Gordin, T. Xu, S. Chen, Z. Yu et al., *Angew. Chem. Int. Ed.* **2015**, *54*, 4325 – 4329; *Angew. Chem.* **2015**, *127*, 4399 – 4403; d) P. Hong Jie, H. Ting Zheng, Z. Qiang, H. Jia Qi, C. Xin Bing et al., *Adv. Mater. Interfaces* **2014**, *1*, 1400227.

[5] a) F. Wu, J. Chen, R. Chen, S. Wu, L. Li et al., *J. Phys. Chem. C* **2011**, *115*, 6057 – 6063; b) G. C. Li, G. R. Li, S. H. Ye, X. P. Gao, *Adv. Energy Mater.* **2012**, *2*, 1238 – 1245; c) M. Sun, S. Zhang, T. Jiang, L. Zhang, J. Yu, *Electrochem. Commun.* **2008**, *10*, 1819 – 1822; d) Y. Yang, G. Yu, J. J. Cha, H. Wu, M. Vosgueritchian et al., *ACS Nano* **2011**, *5*, 9187 – 9193; e) W. Li, Q. Zhang, G. Zheng, Z. W. Seh, H. Yao et al., *Nano Lett.* **2013**, *13*, 5534 – 5540; f) Z. W. Seh, Q. Zhang, W. Li, G. Zheng, H. Yao et al., *Chem. Sci.* **2013**, *4*, 3673 – 3677.

[6] a) Q. Fan, W. Liu, Z. Weng, Y. Sun, H. Wang, *J. Am. Chem. Soc.* **2015**, *137*, 12946 – 12953; b) Z. Zhang, Q. Li, S. Jiang, K. Zhang, Y. Lai et al., *Chem. Eur. J.* **2015**, *21*, 1343 – 1349; c) Z. Wei Seh, W. Li, J. J. Cha, G. Zheng, Y. Yang et al., *Nat. Commun.* **2013**, *4*, 1331; d) X. Tao, J. Wang, C. Liu, H. Wang, H. Yao et al., *Nat. Commun.* **2016**, *7*, 11203.

[7] a) Q. Zhang, Y. Wang, Z. W. Seh, Z. Fu, R. Zhang et al., *Nano Lett.* **2015**, *15*, 3780 – 3786; b) Z. Yuan, H. J. Peng, T. Z. Hou, J. Q. Huang, C. M. Chen et al., *Nano Lett.* **2016**, *16*, 519 – 527; c) Z. W. Seh, J. H. Yu, W. Li, P. C. Hsu, H. Wang et al., *Nat. Commun.* **2014**, *5*, 5017.

[8] Q. Pang, D. Kundu, M. Cuisinier, L. F. Nazar, *Nat. Commun.* **2014**, *5*, 4759.

[9] W. Ai, Z. Z. Du, J. Q. Liu, F. Zhao, M. D. Yi, et al., *RSC Adv.* **2012**, *2*, 12204 – 12209.

[10] a) C. Jin, J. Lee, E. Lee, E. Hwang, H. Lee, *Chem. Commun.* **2012**, *48*, 4235 – 4237; b) Y. Lu, Y. Jiang, H. Wu, W. Chen, *Electrochim. Acta* **2015**, *156*, 267 – 273; c) L. Fan, Q. Zhang, K. Wang, F. Li, L. Niu, *J. Mater. Chem.* **2012**, *22*, 6165 – 6170.

[11] a) K. Deng, J. Zhou, X. Li, *Electrochim. Acta* **2013**, *95*, 18 – 23; b) X. Yang, Y. Lu, Y. Ma, Y. Li, F. Du et al., *Chem. Phys. Lett.* **2006**, *420*, 416 – 420.

[12] O. C. Compton, B. Jain, D. A. Dikin, A. Abouimrane, K. Amine et al., *ACS Nano* **2011**, *5*, 4380 – 4391.

[13] L. Ji, M. Rao, H. Zheng, L. Zhang, Y. Li et al., *J. Am. Chem. Soc.* **2011**, *133*, 18522 – 18525.

[14] H. J. Shin, K. K. Kim, A. Benayad, S. M. Yoon, H. K. Park et al., *Adv. Funct. Mater.* **2009**, *19*, 1987 – 1992.

[15] a) Z. Chenxi, M. Arumugam, *Adv. Energy Mater.* **2013**, *3*, 1008 – 1012; b) X. Yang, L. Zhang, F. Zhang, Y. Huang, Y. Chen, *ACS Nano* **2014**, *8*, 5208 – 5215.

[16] a) H. Chen, C. Wang, W. Dong, W. Lu, Z. Du et al., *Nano Lett.* **2015**, *15*, 798 – 802; b) S. Yuan, Z. Guo, L. Wang, S. Hu, Y. Wang et al., *Adv. Sci.* **2015**, *2*, 1500071.

[17] X. Liang, C. Hart, Q. Pang, A. Garsuch, T. Weiss et al., *Nat. Commun.* **2015**, *6*, 5682.

[18] A. Irigoras, J. M. Mercero, I. Silanes, J. M. Ugalde, *J. Am. Chem. Soc.* **2001**, *123*, 5040 – 5043.

[19] a) A. H. Ilkhechi, M. Scheibitz, M. Bolte, H. W. Lerner, M. Wagner, *Polyhedron* **2004**, *23*, 2597 – 2604; b) A. H. Ilkhechi, J. M. Mercero, I. Silanes, M. Bolte, M. Scheibitz et al., *J. Am. Chem. Soc.* **2005**, *127*, 10656 – 10666; c) L. Kaufmann, H. Vitze, M. Bolte, H. W. Lerner, M. Wagner, *Organometallics* **2007**, *26*, 1771 – 1776; d) N. Sharma, J. K. Ajay, K. Venkatasubbaiah, U. Lourderaj, *Phys. Chem. Chem. Phys.* **2015**, *17*, 22204 – 22209.

Received: September 18, 2016
Revised: October 2, 2016
Published online: October 25, 2016

